Q-factor measurements through injection locking of a semiconductor-glass hybrid laser with unknown intracavity losses

Y. Fan,[1,*] R. M. Oldenbeuving,[1,2] M. R. H. Khan,[3] C. G. H. Roeloffzen,[3] E. J. Klein,[4] C. J. Lee,[1,5,6] H. L. Offerhaus,[7] and K.-J. Boller[1]

[1]*Laser Physics and Nonlinear Optics group, MESA+ Research Institute for Nanotechnology, University of Twente, Enschede 7500 AE, The Netherlands*

[2]*SATRAX B.V., Enschede 7521, The Netherlands*

[3]*Telecommunication Engineering Group, University of Twente, Enschede 7500 AE, The Netherlands*

[4]*XiO Photonics B.V., Enschede 7500 BG, The Netherlands*

[5]*XUV Optics group, MESA+ Research Institute for Nanotechnology, University of Twente, 7500 AE, The Netherlands*

[6]*FOM Institute DIFFER, Nieuwegein 3430BE, The Netherlands*

[7]*Optical Sciences group, MESA+ Research Institute for Nanotechnology, University of Twente, Enschede 7500 AE, The Netherlands*

**Corresponding author: y.fan@utwente.nl*

Received January 7, 2014; revised February 17, 2014; accepted February 17, 2014; posted February 21, 2014 (Doc. ID 203770); published March 19, 2014

The injection locking properties of a newly developed waveguide-based external cavity semiconductor laser have been investigated. Using the injection locking properties to measure the Q-factor of complex optical cavities with unknown internal losses, has been demonstrated for the first time. © 2014 Optical Society of America

OCIS codes: (130.2755) Glass waveguides; (130.3120) Integrated optics devices; (140.5960) Semiconductor lasers; (250.5300) Photonic integrated circuits.

http://dx.doi.org/10.1364/OL.39.001748

Injection locking of lasers is a powerful method for all-optical control of the frequency and phase of laser oscillators with superior precision [1,2]. Semiconductor lasers are a very important target for injection locking, as evidenced by a wide range of fundamental physics applications. These include the generation of nonclassical, sub-Poissonian states of light [3,4], or highly frequency selective amplification in precision metrology based on optical frequency combs [5]. Injection locking of semiconductor lasers is also of great technological importance in integrated optical systems. Examples are the generation of ultrawide tunable radiation (microwave to terahertz) [6], phase locking of entire arrays of lasers [7], phase control of terahertz lasers [8], applications in coherent communications systems [9], and microwave photonics [10].

Emerging hybrid photonic integration, which can combine lasers, splitters, modulators, and detectors on the same substrate, are interesting for a range of applications [11]. Of particular interest is the integration of optical components with complementary (i.e., active versus passive) properties [12] because this can strongly enhance the spectral and temporal control of the generated light, such as via integrated high-Q resonators and delay lines. An example is the integration of InP semiconductor optical amplifiers (SOAs) with spectrally selective Si waveguide resonators for external feedback. This approach yielded integrated external cavity diode lasers with wide spectral tuning [13] and narrow spectral bandwidth [14]. The narrowest spectral bandwidth obtained so far with such waveguide-based external cavity semiconductor lasers (WECSLs) was achieved with using, for the first time, a glass-based waveguide circuit to form a hybrid semiconductor-glass laser. The narrow spectral bandwidth was the result of using feedback from a low-loss glass (Si_3N_4/SiO_2) waveguide circuit containing two microring resonators (MRRs), as shown in Fig. 1. We found, interestingly, that the WECSL had a spectral bandwidth as low as 25 KHz [15]. Nevertheless, the full potential of such lasers is far from being explored.

The low reported spectral bandwidth is likely to be due to the low losses obtained from the glass waveguides [16,17]. These losses make ultralow spectral bandwidths in the subkilohertz range appear feasible if the quality factor (Q-factor) of the WECSL cavity can be increased. This could be achieved by reducing the coupling loss at the interface between the SOA and the waveguide feedback chip, for example. Increasing the Q-factor also yields an inversely proportional narrowing of the locking range [18], which enhances the frequency selectivity of a WECSL. Frequency selective amplification is of great

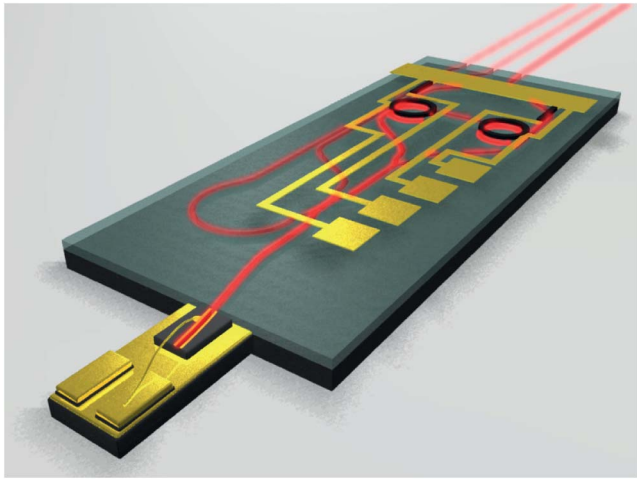

Fig. 1. Schematic structure of the WECSL (not to scale).

interest for the amplification of single lines in optical frequency combs, or narrow sidebands, as is required for phased array antenna applications [19]. This reasoning, however, can be reversed: the inversely proportional relationship between the Q-factor and locking range also enables a direct measurement of the Q-factor of the WECSL cavity. This is important because measuring the round-trip losses in a WECSL is even more difficult than determining the losses in a solitary diode laser [20]. The WECSL is based on a complex cavity, consisting of a low-Q semiconductor gain section and dedicated high-Q waveguide circuitry. In this case, a conventional cavity ring-down measurement cannot be easily conducted [21]. In addition, the need for a laser with a frequency that is on resonance with the WECSL cavity further renders this method prohibitive. An alternative solution might involve measuring the losses originating from numerous mechanisms in a hybrid device. This would require measuring internal losses in the active region [20], propagation loss in the waveguide, and bending losses within each MRR [22], as well as *a priori* unknown feedback and coupling loss at the interface between the SOA and the waveguide chip [23]. This would be time consuming, and large uncertainties would arise due to differences, associated with fabrication and processing variability, between samples used for each measurement.

In this Letter, we demonstrate the first injection locking of a WECSL and characterize its basic parameters. Locking is performed by injecting an RF sideband from a second WECSL. The locking range, measured versus the injected power, is in agreement with previously estimated values for the Q-factor of the WECSL cavity and, thereby, confirms the high potential of WECSLs as new class of integrated-optics oscillators with ultralow bandwidth. The locking demonstrated here also provides a new tool for measuring the cavity Q-factor of WECSLs in operation and, thereby, allows the quality of chip-to-chip coupling to be assessed. The availability of such a tool lies at the heart of hybrid photonic integration involving optical amplification, because measurement of chip-to-chip coupling performance is necessary to guide loss reduction strategies, such as waveguide tapering for spot-size conversion [24].

To recall the essential properties of injection locking: the output from a first laser, called the master laser (ML), is injected into a second laser, called the slave laser (SL). If the detuning of the ML frequency, ν_{ML}, from the free-running SL frequency, ν_{SL}, is smaller than the so-called locking range, i.e., $\Delta\nu_{\mathrm{lk}} > |\nu_{\mathrm{ML}} - \nu_{\mathrm{SL}}|$, the SL starts oscillating at the injected ML frequency rather than at ν_{SL}.

The full locking range, which is twice the so-called locking half-range, is given by [18]

$$\Delta\nu_{\mathrm{lk}} = \frac{\nu_{\mathrm{SL}}}{Q}\sqrt{\frac{P_i}{P_{\mathrm{SL}}}}, \tag{1}$$

where Q is the quality factor of the SL's resonator, P_{SL} is the free running output power, and P_i is the injected power. The latter includes transmission and mode matching losses and is, thus, only a fraction of the ML total output power.

This expression would underestimate the locking range by a factor of $(1+\alpha^2)^{1/2}$ if applied to a solitary diode laser, [25], where α is the linewidth enhancement or Henry factor [26]. In a WECSL, however, only a small fraction of the cavity, $f_c < 1$, is fabricated from semiconductor material. In our case, the light only spends $f_c = 0.15$ of the round-trip time in the semiconductor material, and α is between 3 and 4, according to the manufacturer (Fraunhofer Heinrich-Hertz-Institut, Berlin). Using these considerations, we estimate that the broadening of the locking range is limited to $(1+(f_c\alpha)^2)^{1/2}$, which is in the range of 1.1–1.17 for the WECSLs described here.

Equation (1) can be used to determine the effective Q-factor of the hybrid cavity by varying the injected power and measuring the locking range. The schematic structure of the two WECSLs used is shown in Fig. 1. Both the ML and SL WECSLs are the same as that described in detail in [15]. In brief, the lasers are based on InP SOAs with a nominal output power of 7.4 mW (at drive current 90 mA) at a wavelength of around 1.55 μm. The gain waveguide is tilted at 5 deg with respect to the antireflection-coated output facet. The frequency selective waveguide feedback circuits are fabricated using Si_3N_4/SiO_2 waveguide technology with a box-shaped waveguide cross section [16]. Light coupled into the input/output waveguide travels via a Y-junction through two sequential MRRs (radii of 50 and 55 μm) before traveling back into the SOA. The input–output facet the waveguide is tilted and antireflection coated to minimize coupling losses. Heaters are placed on top of the MRRs to thermally tune the two MRR's resonance frequencies. Output from the WECSLs is obtained after a second Y-junction behind the MRRs.

The injection locking experimental setup is shown in Fig. 2. The light from the ML is coupled into a single-mode fiber and amplified by an erbium-doped fiber amplifier (EDFA, Firmstein Technologies PR25R), followed by a 90/10 splitter. The higher power portion is used to provide the reference signal for heterodyne detection, while the lower power signal is used for injection locking. The injection signal is passed through a Mach–Zehnder optical modulator (Avanex PowerLog FA 20), which is

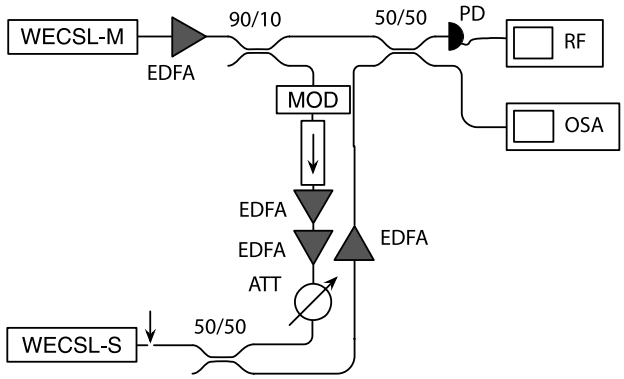

Fig. 2. Schematic of the injection locking setup. The ML is marked as *WECSL-M*; slave, *WECSL-S;* optical modulator, *MOD*; optical isolator, →; optical attenuator, *Att*; couplers, 50/50 and 90/10; optical spectrum analyzer, *OSA;* photodiode, *PD;* and RF spectrum analyzer, *RF*. Measurements of the injected ML power and the SL output power are performed at the location marked with the arrow.

driven by a signal generator (Agilent Technologies E8267D) that is capable of sweeping the modulation frequency, Ω, from 0 to 20 GHz. After modulation, about 15% of the optical power is contained in the first ($\nu_{ML} - \Omega$) sideband. To prevent feedback from the SL into the ML, the modulated signal is passed through an optical isolator (IO-H-1550FC Thorlabs). Thereafter, the injection signal is amplified by two EDFAs (Alcatel 1686WM). The injected power is controlled via a variable attenuator (Ando AQ3105), and the light is injected into the SL via a 50/50 coupler.

This coupler is also the output port of the SL. The output of the SL exits the coupler, and is amplified by an EDFA (Firmstein Technologies PR25R). Following amplification, the SL output is mixed with the reference using a second 50/50 coupler. Half of the light is detected at one port of the 50/50 coupler using a photodiode (Discovery Semi DSC 30S) with a bandwidth of 20 GHz. The beat frequency is recorded using an RF spectrum analyzer (Agilent Signal Analyzer MXA N9020A, maximum range 10 Hz to 26.5 GHz). The light from the second output of the 50/50 coupler is directed to an optical spectrum analyzer (Ando AQ6317, spectral resolution 3 GHz).

The two WECSLs were coarsely tuned until their frequencies were within 20 GHz of each other, as measured by the optical spectrum analyzer. The modulation frequency was then swept so that the frequency of the light injected into the SL was precisely controlled compared to the precision achieved via thermally tuning the ML. The frequency range over which the ML could successfully injection lock the SL was recorded for different injected powers.

To calibrate the power of the injected sideband, we determined the ML power at the output of the 50/50 coupler in front of the SL, which is marked with an arrow in Fig. 2. We measured a ML power of 2.69 mW with the attenuator set to 0 dB, which corresponds to a sideband power of 403.5 μW. At the same position, the output power of the SL was measured to be $P_{SL} = 20.9$ μW. The mode field diameter of the single-mode fiber is specified to be 10.5 ± 0.8 μm (P1-1550PM-FC-2) and that of the waveguide chip is measured to be 1 μm in both directions, yielding a calculated coupling efficiency of 3.56×10^{-2} with uncertainties of −13% and +17%. This allows us to determine the ratio of P_i and P_{SL} in Eq. (1). Using the calculated coupling efficiency, the maximum injected sideband power from the ML was calculated to be $P_i = 14.38$ μW at 0 dB of attenuation.

A set of typical RF spectra is shown in Fig. 3, recorded for different values of the modulation frequency. The presence of injection locking is determined by inspecting the spectra for the number of frequencies of beat notes. If the SL was successfully locked to the ML, a single beat frequency between the reference and locked sideband was observed [see Figs. 3(b)–3(e)]. If the SL was not locked while the frequency of the ML frequency was close to the edge of the locking range, multiple sidebands were observed [see Figs. 3(a) and 3(f)]. The origin of these sidebands is known to be caused by frequency modulation of the intracavity light field, which is induced by the injected light [27].

Figure 4 shows the main result, which is the measured injection locking range as a function of the injected ML

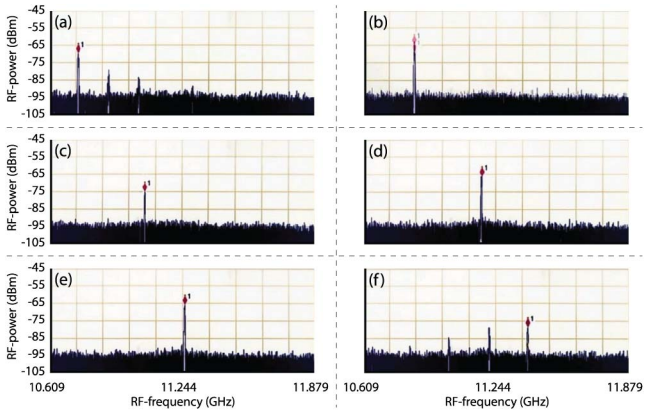

Fig. 3. RF beat spectra of the injected and the SL frequency, recorded for different detunings of the injected ML sideband. Locking is indicated by a single beat frequency [(b)–(e)]. No locking is indicated by the presence of several beat frequencies, generated by the different frequencies of the sideband, reference, and SL [(a) and (f)]. The shown spectra are obtained with an injected power of 14.38 μW. The shown spectra are all centered at 11.24 GHz.

sideband power. The injected powers for which locking was observed range from 6.42 to 14.38 μW. The vertical error bars indicate the experimental uncertainty.

The data is plotted on a double-logarithmic scale in order to investigate whether they follow a linear function with a slope of −1/2 as predicted by Eq. (1). The solid line shows a least-square fit of Eq. (1) to the data, with Q the only free parameter. The best fit value for Q was found to be $(6.2 \pm 1.6) \times 10^4$. The uncertainty comes from two sources: the uncertainty in the locking range, which contributes 1.0×10^4, and might be decreased substantially by using an optimized choice of RF spectrum analyzer and RF modulator sweep times. We address the remaining 0.6×10^4 error to the input power measurements. Taking into account the influence of the Henry factor (10%–17%), the Q is found to be in the range of 4.1×10^4 to 8.6×10^4. We note that this value is of the same order as previous estimates of the Q ($Q = 1.6 \times 10^4$)

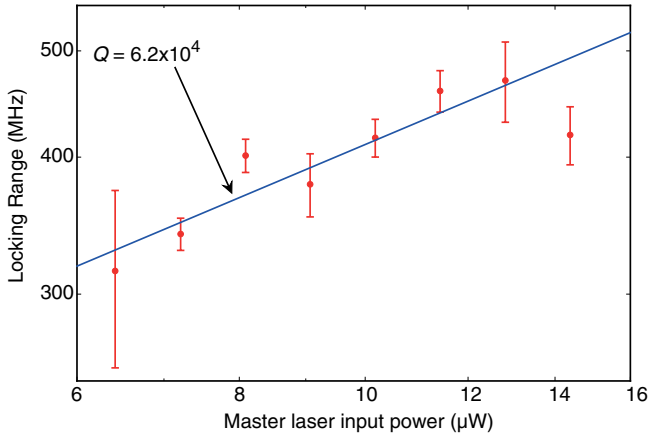

Fig. 4. Injection locking range of the WECSL versus the injected sideband power, on a double-logarithmic scale. The output power of the locked SL-WECSL is 0.587 mW. The red circles depict the experimental data. The solid line is a least-squares fit of Eq. (1) with Q as the only free parameter.

based on an estimated 13.5 ps photon lifetime in the WECSL cavity [15].

Here, we have investigated injection locking of a novel type of hybrid laser based on semiconductor gain and glass waveguide feedback. Integrated optical lasers lend themselves to injection locking because they are largely immune to mechanical perturbations and drifts of mode-matching conditions. This ease of injection locking allows it to be used as a method to quantify the effective Q-factor of integrated optical cavities with unknown internal losses. This tool may also be used to inspect the intracavity losses of standard monolithic diode lasers, such as Fabry–Perot and distributed feedback lasers.

This research is supported by the Dutch Technology Foundation STW, which is part of the Netherlands Organization for Scientific Research (NWO) (project no. 10442), and partly supported by funding within the framework of the Promis2Day project, for which the authors gratefully acknowledge the support of the IOP Photonic Devices program of Agentschap NL, part of the Netherlands Ministry of Economic Affairs and the Netherlands Ministry of Education, Culture and Science.

References

1. H. L. Stover, Appl. Phys. Lett. **8**, 91 (1966).
2. C. J. Buczek, R. J. Freiberg, and M. L. Skolnick, Proc. IEEE **61**, 1411 (1973).
3. H. Wang, M. J. Freeman, and D. G. Steel, Phys. Rev. Lett. **71**, 3951 (1993).
4. S. Kasapi, S. Lathi, and Y. Yamamoto, Opt. Lett. **22**, 478 (1997).
5. T. Fortier, Y. Le Coq, J. Stalnaker, D. Ortega, S. Diddams, C. Oates, and L. Hollberg, Phys. Rev. Lett. **97**, 163905 (2006).
6. G. J. Schneider, J. A. Murakowski, C. A. Schuetz, S. Shi, and D. W. Prather, Nat. Photonics **7**, 118 (2013).
7. L. Goldberg, H. F. Taylor, J. F. Weller, and D. M. Bloom, Electron. Lett. **19**, 491 (1983).
8. D. Oustinov, N. Jukam, R. Rungsawang, J. Madéo, S. Barbieri, P. Filloux, C. Sirtori, X. Marcadet, J. Tignon, and S. Dhillon, Nat. Commun. **1**, 1 (2010).
9. T. Jung, J.-L. Shen, D. T. K. Tong, S. Murthy, M. C. Wu, T. Tanbun-Ek, W. Wang, R. Lodenkamper, R. Davis, L. J. Lembo, and J. C. Brock, IEEE Trans. Microw. Theor. Technol. **47**, 1225 (1999).
10. J. Capmany and D. Novak, Nat. Photonics **1**, 319 (2007).
11. Y. Urino, T. Shimizu, M. Okano, N. Hatori, M. Ishizaka, T. Yamamoto, T. Baba, T. Akagawa, S. Akiyama, T. Usuki, D. Okamoto, M. Miura, M. Noguchi, J. Fujikata, D. Shimura, H. Okayama, T. Tsuchizawa, T. Watanabe, K. Yamada, S. Itabashi, E. Saito, T. Nakamura, and Y. Arakawa, Opt. Express **19**, B159 (2011).
12. Y. Wakayama, T. Kita, and H. Yamada, Jpn. J. Appl. Phys. **50**, 04DG20 (2011).
13. S. Tanaka, S.-H. Jeong, S. Sekiguchi, T. Kurahashi, Y. Tanaka, and K. Morito, Opt. Express **20**, 28057 (2012).
14. K. Nemoto, T. Kita, and H. Yamada, Appl. Phys. Express **5**, 082701 (2012).
15. R. M. Oldenbeuving, E. J. Klein, H. L. Offerhaus, C. J. Lee, H. Song, and K.-J. Boller, Laser Phys. Lett. **10**, 015804 (2013).
16. F. Morichetti, A. Melloni, M. Martinelli, R. G. C. Heideman, A. Leinse, D. H. Geuzebroek, and A. Borreman, J. Lightwave Technol. **25**, 2579 (2007).
17. J. F. Bauters, M. J. R. Heck, D. D. John, J. S. Barton, C. M. Bruinink, A. Leinse, R. G. Heideman, D. J. Blumenthal, and J. E. Bowers, Opt. Express **19**, 24090 (2011).
18. R. Adler, Proc. IRE **34**, 351 (1946).
19. A. Meijerink, C. G. H. Roeloffzen, R. Meijerink, L. Zhuang, D. A. I. Marpaung, M. J. Bentum, M. Burla, J. Verpoorte, P. Jorna, A. Hulzinga, and W. van Etten, J. Lightwave Technol. **28**, 3 (2010).
20. P. A. Andrekson, N. A. Olsson, T. Tanbun-Ek, R. A. Logan, D. Coblentz, and H. Temkin, Electron. Lett. **28**, 171 (1992).
21. S. L. Logunov, Appl. Opt. **40**, 1570 (2001).
22. Y. Vlasov and S. McNab, Opt. Express **12**, 1622 (2004).
23. Y. Barbarin, E. Bente, C. Marquet, E. Leclere, J. Binsma, and M. K. Smit, IEEE Photon. Technol. Lett. **17**, 2265 (2005).
24. T. Mizuno, T. Kitoh, M. Itoh, T. Saida, T. Shibata, and Y. Hibino, J. Lightwave Technol. **22**, 833 (2004).
25. F. Mogensen, H. Olesen, and G. Jacobsen, IEEE J. Quantum Electron. **21**, 784 (1985).
26. C. Henry, IEEE J. Quantum Electron. **18**, 259 (1982).
27. A. E. Siegman, *Lasers*, 1st ed. (University Science Books, 1986).